

# On the Plastic Constraint Factor of Polymers

Ralf Lach,<sup>1</sup> Patricia M. Frontini,<sup>2</sup> Wolfgang Grellmann\*<sup>1,3</sup>

**Summary:** The plastic constraint factor based on Hill's theory of plasticity is widely used to check the stress state applying the essential-work-of-fracture (EWF) approach to polymers. However, the plastic constraint factor experimentally determined as the ratio of the net section stress in cracked specimens and the yield stress does not match the theoretical predictions of the theory of plasticity because assuming ideal-plastic behaviour for polymer materials does not consider material-specific viscoelastic–viscoplastic effects adequately. Therefore, a correction term for amorphous thermoplastic polymer materials is derived introducing the influence of the material on the plastic constraint factor. This correction term is based on the Williams-Landel-Ferry (WLF) equation for different thermodynamic quantities such as temperature and stress (negative pressure) and the introduction of a glass stress to be comparable to the glass temperature. Analytical calculation of this correction term, taking polycarbonate as an example, is used as a comparison to empirical values in literature for numerous amorphous and semi-crystalline thermoplastic as well as partial-plastically deformable elastomeric polymer materials. It can be concluded that this enhanced Hill's theory is well suited to amorphous polymers.

**Keywords:** essential-work-of-fracture approach; Hill's theory of plasticity; plastic constraint factor; viscoelastic–viscoplastic effects; Williams-Landel-Ferry equation

## Introduction

Fracture toughness of ductile polymers under plane stress can be determined using the essential-work-of-fracture (EWF) method. Based on the pioneering work of Broberg,<sup>[1]</sup> Cotterell and Reddel,<sup>[2]</sup> and Mai and Cotterell<sup>[3]</sup> a large number of related papers has been published since that time extensively reviewed by Barany, Czigany and Karger-Kocsis in 2010.<sup>[4]</sup> However, to apply the EWF method adequately it must be provided that certain specific requirements are met.<sup>[5,6]</sup> In such a case a linear relationship between work of

fracture and ligament length exists according to Figure 1. One important factor influencing the applicability of this procedure is the stress state in the ligament length. For ligament lengths much longer than the sample thickness, ductile polymers will always be in a state of pure plane stress. This assumption can be experimentally checked by measuring the net stress in the ligament at the point of full yielding. One of the mean criteria for applying the fracture mechanics approach of EWF in a correct way can be derived from checking the present stress state, i.e. generally, if pure plane stress state exists (Figure 1). In this regard, the plastic constraint factor  $m$  based on Hill's theory<sup>[7]</sup> of plasticity is widely applied. As an example, values of  $m = 1$  for single-edge notched tensile (SENT) specimens and  $m = 1.15$  for double-edge notched tensile (DENT) specimens should be hypothesised for ideal-plastic material behaviour and plane stress state. However,  $m$  values that are

<sup>1</sup> Polymer Service GmbH Merseburg, Eberhard-Leibnitz-Straße 2, 06217 Merseburg, Germany  
E-mail: wolfgang.grellmann@psm-merseburg.de

<sup>2</sup> Universidad Nacional del Mar de Plata, Materials Science and Technology Research Institute (INTEMA), Avenida Juan B. Justo 4302, B7608FDQ Mar del Plata, Argentina

<sup>3</sup> Martin Luther University Halle-Wittenberg, Centre of Engineering, 06099 Halle, Germany

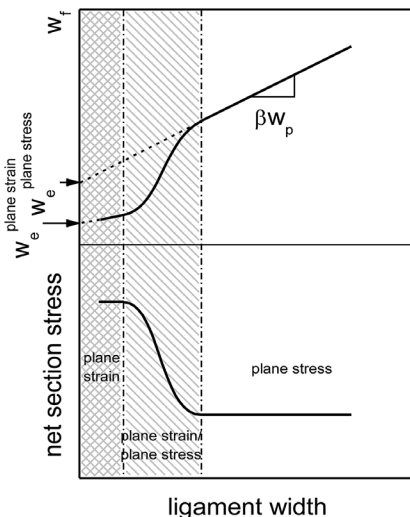


**Figure 1.**

Influence of the ligament width and the related change in stress state on the specific work of fracture  $w_f$  and the flow stress ("net section stress") in cracked specimens;  $w_e^{\text{plane strain}}$  and  $w_e^{\text{plane stress}}$  – essential-work-of-fracture (EWF) both for plane strain and plane stress state,  $w_p$  – specific plastic work of fracture for plane stress state,  $\beta$  – shape factor of the plastic zone.

smaller than  $m = 1$  or  $m = 1.15$  are often observed for non-elastomeric polymer materials also in spite of the existence of the plane stress state because the assumption of ideal-plastic behaviour for all polymers is not strictly valid in comparison to other materials such as ductile metals. In the following section, "Theoretical considerations", a correction term for amorphous thermoplastic polymer materials is derived, therefore introducing the influence of the material on  $m$ . Subsequently, in the section "Applications" the analytical calculation of this correction term, taking polycarbonate as an example, is used as a comparison to empirical values in literature for numerous amorphous and semi-crystalline thermoplastic as well as partial-plastically deformable elastomeric polymer materials.

## Theoretical Considerations

For amorphous thermoplastic polymer materials, linear viscoelastic behaviour is generally the dominant one in the

linear-response region, while non-linear viscoelastic–viscoplastic material behaviour takes increasingly effect at higher stresses. This behaviour has to be considered in connection with the specific molecular structure of these materials, although, in comparison to viscoelastic–viscoplastic materials having an atomic structure such as aluminium. Several characteristics resulting from this macromolecular structure of polymers also strongly affect their fracture behaviour. As an example, in compact specimens at impact bending loading crack initiation is observed at stresses that are much smaller than the maximum stress, which does not occur in metallic materials. The determination of the plastic constraint factor enables the analysis of the influence of specimen geometry, stress state and material on the flow stress or the stress at crack initiation in cracked specimens. Under certain conditions, a global stress analysis can be applied for mechanically homogeneous polymers (PC, PS, PMMA, SAN etc.), while a local stress analysis is required for mechanically heterogeneous polymer materials (such as multi-component materials: ABS, PS-HI, etc.) without restricting the universality of the following derivations.

At continuously increased stress such as applied during uniaxial tensile testing a highly co-operative level of movement should be obtained corresponding to the stress  $\sigma_0$  that is smaller than or – at higher temperatures  $T \approx T_g$  – equal to the yield stress at the most, so that  $\sigma_0$  can be designated as "glass stress"<sup>1</sup> analogous to the glass temperature  $T_g$  (Figure 2). This

<sup>1</sup>Due to the replaceability of the thermodynamic quantities temperature  $T$  and pressure  $p$  in the WLF equation (Equation (1a) and (1b)) the glass transition can be determined in different ways, (i) by varying the temperature at constant pressure (or stress  $\sigma$ ) and (ii) by varying the pressure (or stress  $\sigma$ ) at constant temperature. The first way (i) to be the most common one results in determination of  $T_g(\sigma)$ . The second way (ii) to be more rarely realised results in determination of  $\sigma_0(T)$  (see Figure 2). Thus, analogously to  $T_g$  as the glass (transition) temperature,  $\sigma_0$  is introduced here as "glass stress".

assumption can be substantiated polymer-physically by the fluctuation–dissipation theorem. Also at uniaxial loading the external stress takes partly effect in form of dilatation stress because the Poisson’s ratio for thermoplastics is smaller than 0.5 at  $T < T_g$  (plane strain state uniaxial loading conditions always lead to dilatation stresses, also if Poisson’s ratio = 0.5). In doing so, free volume is induced, which results in increasing mobility of the macromolecules or parts of them and finally in increasing energy dissipation. (On this basis it may be assumed that the mechanical loss factor – determined by superposition of a small sinus-shaped time-dependent stress and a pre-stress  $\sigma$  – should pass through a maximum at  $\sigma = \sigma_0$ .) This behaviour results in a hyperbolic-shaped temperature dependence of  $\sigma_0 = \sigma_0(T)$  (Equation (1c)) which can be derived from comparisons of formulations of the Williams-Landel-Ferry (WLF) equation<sup>[8]</sup> for different thermodynamic quantities such as temperature  $T$ <sup>[9,10]</sup> (Equation (1a))

$$\ln \left[ \frac{\Psi}{f}(T, p) \right] \cdot [T - T_\infty(p)] = \ln \left[ \frac{\Psi}{f_{\text{ref}}}(T_{\text{ref}}, p) \right] \cdot [T_{\text{ref}} - T_\infty(p)] \quad (1a)$$

[ $f$  – frequency,  $\Psi$  – high-frequency asymptote, i.e. maximum relaxation frequency of local regions of the macromolecule (for glass transition of polymers:

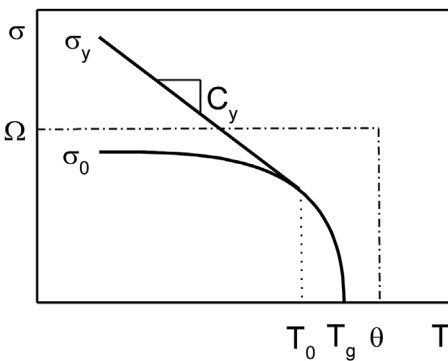


**Figure 2.** Temperature dependence of the “glass stress”  $\sigma_0$  and the yield stress  $\sigma_y$ ; for further information: see text.

$\Psi \approx 10^{13} \text{ Hz}^{[10]}$ ,  $T_\infty$  – Vogel temperature, ( $f_{\text{ref}}, T_{\text{ref}}$ ) – reference point] and pressure  $p$ <sup>[9,10]</sup> (Equation (1b))

$$\ln \left[ \frac{\Psi}{f}(T, p) \right] \cdot [p - p_\infty(T)] = \ln \left[ \frac{\Psi}{f_{\text{ref}}}(T, p_{\text{ref}}) \right] \cdot [p_{\text{ref}} - p_\infty(T)] \quad (1b)$$

( $p_\infty$  – “Vogel” pressure, ( $f_{\text{ref}}, p_{\text{ref}}$ ) – reference point). The pressure can also occur in form of stress, i.e. “negative” pressure, with  $\sigma = -p$ <sup>[10]</sup>:

$$\sigma_0 = \Omega + \frac{C}{T - \theta} \quad (1c)$$

( $\Omega$  – stress (pressure) asymptote depending on the material and the type of loading,  $\theta$  – material-dependent temperature asymptote,  $C$  – empirical parameter).

Assuming that the stresses in the material become small at the glass temperature  $T_g$  compared to the glassy state, i.e.

$$\sigma_0|_{T-T_g} \approx 0, \quad (2)$$

it follows

$$\sigma_0 \approx \Omega \frac{T - T_g}{T - \theta}. \quad (3)$$

For craze-forming materials, the stress  $\sigma_0$  is identical with the so-called craze stress.<sup>[11,12]</sup>

However, motion processes resulting in wide-ranging plastic deformations (in the sense of non-affine deformations such as the restructuring of the entanglement network) do not have enough time to become fully operative at temperatures much smaller than the glass temperature, i.e.  $T < T_0$ , because the stress in the uniaxial tensile test at deformation rates ranging from about  $0.01 \text{ min}^{-1}$  to about  $1 \text{ min}^{-1}$  is continuously increased through the glass transition point  $\sigma_0$ . These processes are only initiated (formation of micro-shear bands and crazes). For stresses  $\sigma_0 > \sigma > \sigma_y$  (at brittle behaviour for  $\sigma_0 > \sigma > \sigma_y$  stress at break), the mobility of the macromolecules or parts of them is reduced by overstretching individual chains and the corresponding immobilisation of the entanglements. (This process should result in

decreasing mechanical loss factors at prestresses  $\sigma > \sigma_0$ .) The combination of this process with an orientation of the macromolecules can result in strain crystallisation for crystal-forming polymers<sup>[13]</sup> corresponding to a further reduction in the chain mobility. Typically, for many materials, depending on the entanglement density for example, a macroscopic instability can be observed at the so-called yield point ( $\sigma = \sigma_y$ ) where the locally affine deformation changes into a globally affine one.<sup>2</sup> The linear growth of fibrils (“fibril drawing”) in “low-temperature” crazes and the so-called cold drawing process are both characteristics of the phenomenon of the affine deformation in the microscopic ( $\sigma < \sigma_y$  or  $\sigma < \text{stress at break}$ , respectively) and macroscopic ( $\sigma > \sigma_y$ ) scale. Passing the yield point in amorphous polymers may not be misinterpreted as onset of intrinsically plastic (non-affine) deformations, to which investigations by, for example, Karger-Kocsis<sup>[14]</sup> refer. Deformations inside a so-called “plastic” zone generated by cold drawing have been found to be recovered nearly completely after annealing at temperatures little above the glass temperature, because – as described above – this type of deformation only results from orientation of the macromolecules (shift of the entanglements in loading direction). A further indication of the assumption that passing the yield point may be only related with affine deformations is the low cooperativity at  $\sigma > \sigma_y$ . It is well known that the yield stress depends on the strain rate, as described by the Eyring equation that is based on a two-potential well model usually only applied to linear-viscoelastic behaviour (low cooperativity). For this reason, the shape of the temperature dependencies of the yield stress and the glass stress differ from each other.

<sup>2</sup>For materials having only a small entanglement density, only few molecules are over-stretched but highly, stimulating brittle fracture. Furthermore, the large mesh size of the entanglement network promotes micro-cavities (“pre-crazes”) and the formation of crazes<sup>[16]</sup> (compare also Wu<sup>[17]</sup>).

The temperature dependence of the yield stress  $\sigma_y$  is bi-linear – taking polycarbonate as an example – up to temperatures closely below the glass temperature ( $T < T_0$ ). Here, the negative slope  $d\sigma_y/dT$  at temperatures smaller than  $-100^\circ\text{C}$ , i.e. at temperatures smaller than the maximum temperature of the secondary ( $\beta$ ) relaxation process, is smaller than that at higher temperatures.<sup>[15]</sup> In principle, in both temperature ranges

$$\sigma_y = \Omega_y - C_y T, \quad (4)$$

( $\Omega_y$ ,  $C_y$  – empirical parameter) is obtained where, in the following, the high-temperature segment is only of interest. However, such strict correlation of the two segments to the  $\beta$ - and  $\alpha$ -relaxation as stated in<sup>[15]</sup> may be oversimplified due to investigations by Karger-Kocsis<sup>[14]</sup> including our own explanations given above. Except PC, the relationship  $\sigma_y(T)$  described by Equation (4) has been observed also for other polymer materials.

By using the boundary conditions (see Figure 2):

$$\sigma_y|_{T=T_0} = \sigma_0|_{T=T_0}, \quad (5a)$$

$$\left. \frac{d\sigma_y}{dT} \right|_{T=T_0} = \left. \frac{d\sigma_0}{dT} \right|_{T=T_0}, \quad (5b)$$

$T_0$  and  $\Omega$  can be calculated:

$$T_0 = \theta - \sqrt{\frac{\Omega}{C_y}(\theta - T_g)}, \quad (6a)$$

$$\Omega = (\Omega_y - C_y T_0) \frac{T_0 - \theta}{T_0 - T_g}. \quad (6b)$$

In spite of different loading conditions, the value of  $\Omega$  ( $\Omega = 54.3 \text{ MPa}$ ) determined for quasi-static tensile loading in this way is in relatively good agreement with the value of  $\Omega$  ( $\Omega = 45.5 \text{ MPa}$ <sup>[10]</sup>) experimentally determined under impact bending loading.

The chain mobility is high enough only in the temperature range  $T_0 < T < T_g$  to probably prevent over-stretching of the chains combined with immobilisation of the entanglements, so that cavities, for example, can be healed during the time of testing. This prediction is in agreement with

the observation that crazes (crazes I in the meaning of<sup>[18]</sup>) cannot be formed at temperatures little below the glass temperature.<sup>[16]</sup>

Assuming ideal-plastic material behaviour, the influence of notches of the amount of the flow stress  $\sigma_{\max}$  (here:  $\sigma_{\max}^{\text{theo}}$ ) is described by Hill<sup>[7]</sup> using the plastic constraint factor  $m_{\text{Hill}}$ :

$$m_{\text{Hill}} = \frac{\sigma_{\max}^{\text{theo}}}{\sigma_y} \quad (7)$$

The plastic constraint factor  $m_{\text{exp}}$  for non-ideal plastic materials is a multiplication function of the constraint factor  $m_{\text{Hill}}$  related to the specimen configuration and the stress state for ideal-plastic behaviour and a constraint factor (correction factor)  $m_{\text{material}}$  reflecting the specific material behaviour:

$$\begin{aligned} m_{\text{exp}} &= \frac{\sigma_{\max}^{\text{exp}}}{\sigma_y} = m_{\text{Hill}} \cdot m_{\text{material}} \\ &= \frac{\sigma_{\max}^{\text{theo}}}{\sigma_y} \cdot \frac{\sigma_0}{\sigma_y} \end{aligned} \quad (8)$$

Thus,  $m_{\text{material}}$  can be simply determined experimentally or analytically, since  $m_{\text{Hill}}$  is known:

$$m_{\text{material}} = \frac{m_{\text{exp}}}{m_{\text{Hill}}} = \frac{\sigma_0}{\sigma_y} \quad (9)$$

$m_{\text{material}}$  is determined analytically by Equation (9) for  $T \leq T_0$  with  $m_{\text{material}} = \sigma_0/\sigma_y$  and by  $m_{\text{material}} = 1$  for  $T_0 \leq T < T_g$  (compare Figure 2). Above the glass temperature the model cannot be applied (see also section “Applications”).

## Applications

### Experimentally and Analytically Determined Plastic Constraint Factors for Polymer Materials

In Figure 3, the ratio of the experimentally determined plastic constraint factor  $m_{\text{exp}}$  (data from literature) and the plastic constraint factor  $m_{\text{Hill}}$  according to Hill’s theory are shown depending on the yield stress  $\sigma_y$  for different polymer materials. A compilation of the data including related

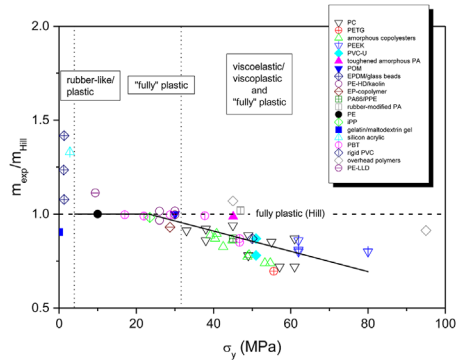


**Figure 3.** Ratio of the experimentally determined plastic constraint factor  $m_{\text{exp}}$  (data from literature) and the plastic constraint factor  $m_{\text{Hill}}$  according to Hill’s theory depending on the yield stress  $\sigma_y$  for different polymer materials (compare also Table 1 with related citations); the solid line illustrates the trend only.

citations is given in Table 1. Depending on the yield stress, three regions can be distinguished in Figure 3 for which different values of the ratio  $m_{\text{exp}}/m_{\text{Hill}}$  are found: For  $\sigma_y < 3$  MPa values of mostly  $m_{\text{exp}}/m_{\text{Hill}} \geq 1$ , for  $3 \text{ MPa} < \sigma_y < 30 \text{ MPa}$  values of  $m_{\text{exp}}/m_{\text{Hill}} \approx 1$  and for  $\sigma_y > 30 \text{ MPa}$  values of  $m_{\text{exp}}/m_{\text{Hill}} \leq 1$ . The occurrence of data points unexpected in the region  $\sigma_y < 3 \text{ MPa}$  (determined exclusively using elastomers) is attributed to the fact that – except thermoplastic materials – also in some elastomeric materials “plastic” deformations are observed. Here, the affine deformation of the polymer network is superimposed by non-affine deformations occurring less distinct as a result of local rupture of some network points (Figure 4).

Whereas  $m_{\text{exp}}/m_{\text{Hill}}$  analytically described by Equation (9) is in good agreement compared to experimental results obtained for polycarbonate (Figure 5a), also in respect of other amorphous polymer materials (Figure 5b), the statements made in the section “Theoretical considerations” cannot be applied to elastomeric and semicrystalline polymer materials. In semicrystalline polymers the amorphous phase remains in the entropy-elastic state and in

**Table 1.**

Plastic constraint factor  $m_{\text{exp}}$  experimentally determined for polymer materials (test temperature was room temperature unless otherwise noted).

Material	Comment	Specimen	$m_{\text{exp}}$	$\sigma_y$ [MPa]	Reference
<b>Amorphous polymer materials</b>					
PC	25 °C	DENT	1	61	[19]
	40 °C		0.98	55	
	60 °C		1.02	49	
	80 °C		1.08	45	
	100 °C		1.06	38	
	120 °C		1.05	33	
	25 °C	SENT	0.72	61	
	60 °C		0.78	49	
	100 °C		0.86	38	
	PC		SENT	0.72	
PETG		DENT	0.8	55.6	[21]
PET		DENT	0.85	54.7	[22,23]
Amorphous copolyesters		DENT	0.89	48.8	[22,23]
			0.85	53.3	
			0.9	49.2	
			0.95	42.5	
			1	40.4	
Copolyester	1 mm/min	DENT	1.02	39.2	[14]
	10 mm/min		1.03	40.8	
	100 mm/min		0.99	44.9	
PBT	25 °C	DENT	1	45.94	[24,25]
		SENT	0.85	46.04	
	40 °C	DENT	1.14	37.73	
	60 °C		1.146	28.78	
	80 °C		1.138	21.97	
	100 °C		1.146	17.01	
Non-crystalline PEEK		SENT	0.81	62	[26]
PVC-U		DENT	1	51	[27]
		SENT	0.78	51	
Rigid PVC		DENT	1	50	[28]
Toughened amorphous PA		DENT	1.135	45.1	[29]
<b>Semicrystalline polymer materials</b>					
PEEK		DENT	0.92	62	[30]
		SENT	0.86	62	
PEEK		SENT	0.8	80	[26]
POM		DENT	1	30	[31]
Overhead polymers		DENT	1.23	45	[32]
			1.05	90	
PE		SENT	1	10	[33]
PE-LLD		DENT	1.28	9.39	[34]
PE-LD	90 $\mu\text{m}$ film	DENT	1.18	8.5	[35]
	180 $\mu\text{m}$ film		1.24	8.5	
PE-HD/20 vol-% kaolin	0.2 mm/min	DENT	1.168	26	[23]
	2 mm/min		1.112	26	
PE-HD/30 vol-% kaolin	0.2 mm/min	DENT	1.169	30	[23]
	2 mm/min		1.147	30	
iPP		DENT	1.13	23.5	[23,36]
EP copolymer		DENT	1.07	28.7	[5]
PA 66/PPE		DENT	1	45	[37]
Rubber-modified PA		DENT	1.17	47	[33]
		SENT	1.02	47	
<b>Elastomeric polymer materials</b>					
EPDM/glass beads		DENT	1.24	1.29	[38]
			1.42	1.2	
			1.63	1.29	
Gelatin/maltodextrin gel		DENT	1.04	0.027	[39]
Silicon acrylic		SENT	1.33	2.8	[40]

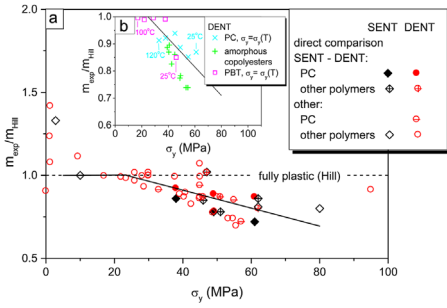


**Figure 4.** Influence of the specimen on the ratio  $m_{exp}/m_{Hill}$  (data of  $m_{exp}$  from literature) as a function of the yield stress  $\sigma_y$  for different polymer materials (compare also Table 1 with related citations) (a); Influence of the temperature (PC,<sup>[9]</sup> PBT<sup>[24,25]</sup>) and the morphology (amorphous copolyesters<sup>[22,23]</sup>) on  $m_{exp}/m_{Hill}(\sigma_y)$  for DENT specimens (b); the solid lines illustrate the trend only.

elastomeric polymers the whole matter at applied temperatures  $T > T_g$  of testing, so that for these materials the derivation given above and the model to calculate  $m_{exp}/m_{Hill}$  by means of the right part of Equation (9), i.e. using  $m_{exp}/m_{Hill} = \sigma_0/\sigma_y$ , cannot be applied. For semicrystalline polymer materials having yield stresses smaller than 60 MPa  $m_{exp}/m_{Hill}$  values of about 1 are assumed (also for yield stresses larger than 60 MPa the values of  $m_{exp}/m_{Hill}$  are larger, as it would be expected for amorphous polymer materials). This corresponds with the observation that for these materials irreversible structural changes – such as due to breakup of crystal lamellae – occur only after passing the yield point, which manifests itself macroscopically in plastic deformations. Also for this reason the material behaviour of some semicrystalline polymers such as PE and PA can be well approximated by assuming ideal-plastic behaviour. The behaviour of such elastomeric materials, which are partly plastically deformable, cannot – as stated above – analytically determined by means of the right part of Equation (9), i.e. using  $m_{exp}/m_{Hill} = \sigma_0/\sigma_y$ . A reason why for elastomers rather larger values of  $m_{exp}/m_{Hill}$  up to  $m_{exp}/m_{Hill} = 1.4$  are found, cannot be given yet.

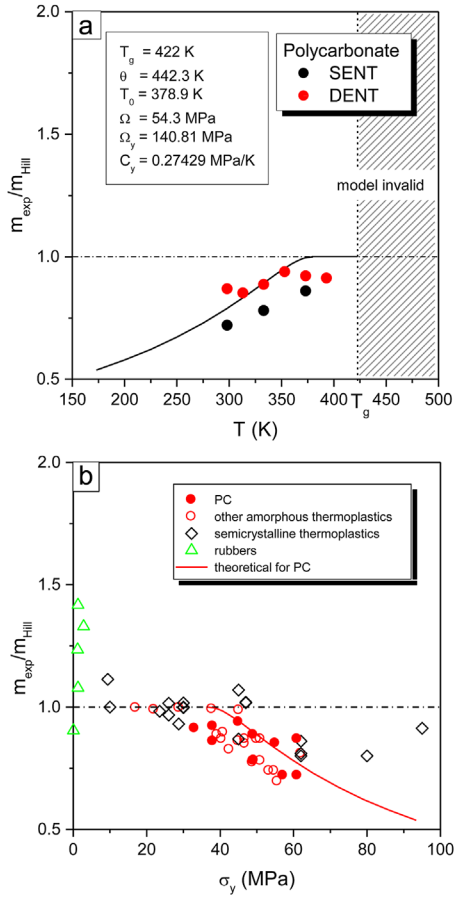


**Figure 5.** Values of  $m_{exp}/m_{Hill}(T)$  calculated according to Equation (9) compared to values experimentally determined for polycarbonate (data from <sup>[9]</sup>) (a); values of  $m_{exp}/m_{Hill}(\sigma_y)$  calculated according to Equation (9) compared to values determined for different polymer materials (values from data in literature; for data including related citations see Table 1) (b); value of  $\theta$  from <sup>[10]</sup>, values of  $T_0$  and  $\Omega$  determined according to Equation (6a) and (6b), values of  $\Omega_y$  and  $C_y$  from fitting Equation (4) to data in <sup>[9]</sup>

**Microplastic Deformations and Crack Initiation Point Depending on the Loading Rate for Polymer Materials**

The following statements shall be also only applied for amorphous polymers in the formulation given here.

For linear-viscoelastic behaviour the time–temperature superposition principle is valid, i.e. large times or low loading rates

$\dot{\varepsilon}$  have the same effect as large temperatures. For non-linear viscoelastic behaviour this principle can be expressed in the form of a three-dimensional relationship between (pre-)stress, temperature and time or rate, i.e., for example, the relationship between glass stress  $\sigma_0$  and temperature depends on the rate (Figure 6). Conversely it applies that the relationship between  $\sigma_0$  and rate depends on temperature. (However, due to their non-linearity both relationships cannot be simply converted into each other (see, [41] for example).) Thus,  $T$  may be replaced with  $1/\ln \dot{\varepsilon}$  in Equation (3). At constant temperature it applies:

$$\sigma_0 = \Omega \frac{1 - \frac{\ln \dot{\varepsilon}}{\ln \dot{\varepsilon}_g}}{1 - \frac{\ln \dot{\varepsilon}}{\ln \dot{\varepsilon}_{lim}}} \quad (10)$$

[ $\dot{\varepsilon}_g$  – rate for  $\sigma_0 = 0$  (glass transition),  $\dot{\varepsilon}_{lim}$  – material-dependent rate asymptote].

At constant temperature, the yield stress  $\sigma_y$  can be calculated using the Eyring equation that can be simplified as follows:

$$\sigma_y = \sigma_{y0} + C_\varepsilon \ln \dot{\varepsilon} \quad (11)$$

( $C_\varepsilon, \sigma_{y0}$  – material constants within well-defined ranges of temperature).

Based on the conditions  $\sigma_y = \sigma_0$  and  $d\sigma_y/d\dot{\varepsilon} = d\sigma_0/d\dot{\varepsilon}$  for  $\dot{\varepsilon} = \dot{\varepsilon}_0$  analogous to

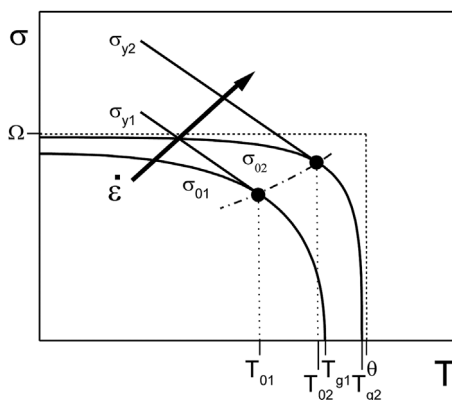


**Figure 6.**

“Glass stress”  $\sigma_{01;02}$  and yield stress  $\sigma_{y1;y2}$  depending on temperature for different loading rates  $\dot{\varepsilon}$ ;  $T_{g1;g2}$  – glass temperatures,  $\Omega, \theta$  – stress and temperature asymptotes.

Equation (5a,b), it follows for  $\Omega$  and  $\dot{\varepsilon}_0$ :

$$\Omega = (\sigma_{y0} + C_\varepsilon \ln \dot{\varepsilon}_0) \frac{1 - \frac{\ln \dot{\varepsilon}_0}{\ln \dot{\varepsilon}_{lim}}}{1 - \frac{\ln \dot{\varepsilon}_0}{\ln \dot{\varepsilon}_g}} \quad (12a)$$

$$\dot{\varepsilon}_0 = \dot{\varepsilon}_{lim} \cdot \exp \left( 1 - \sqrt{\frac{\Omega}{C_\varepsilon} \left( \frac{1}{\ln \dot{\varepsilon}_{lim}} - \frac{1}{\ln \dot{\varepsilon}_g} \right)} \right) \quad (12b)$$

Thus,  $m_{material}$  can be calculated according to Equation (9).

Figure 6 shows schematically that the effect of the material-related constraint factor increases with increasing loading rate. For very high local rates that occur under impact-like loading, for example, this results in initiation of plastic deformation processes in cracked specimens already at very low external stresses and consequently crack initiation at rather small external stresses. A starting point to describe this phenomenon mathematically is given with Equations (10) to (12b) in connection with Equations (7) to (9).

## Conclusions

The plastic constraint factor for viscoelastic–viscoplastic amorphous thermoplastics is found to be a multiplication function of Hill’s constraint factor related to the specimen configuration and the stress state for ideal-plastic behaviour and a correction factor reflecting the specific material behaviour. This correction term was calculated based on the Williams-Landel-Ferry equation for different thermodynamic quantities such as temperature and stress introducing a glass stress to be comparable to the glass temperature. From comparison with experimental data in literature it can be finally concluded that this enhanced theory of plasticity is well suited to amorphous polymers.

## List of Abbreviations

ABS acrylonitrile-butadiene-styrene copolymer



EWf	essential work of fracture
EP	ethylene-propylene
EPDM	ethylene-propylene-diene rubber
DENT	double-edge notched tensile
iPP	isotactic polypropylene
PA	polyamide
PBT	poly(butylene terephthalate)
PC	polycarbonate
PE	polyethylene
PEEK	poly(ether ether ketone)
PE-HD	high-density polyethylene
PE-LD	low-density polyethylene
PE-LLD	linear low-density polyethylene
PET	poly(ethylene terephthalate)
PETG	poly(ethylene terephthalate glycol)
PMMA	poly(methyl methacrylate)
POM	polyoxymethylene
PPE	poly(phenylene ether)
PS	polystyrene
PS-HI	high-impact polystyrene
PVC	poly(vinyl chloride)
PVC-U	unplasticised poly(vinyl chloride)
SAN	styrene-acrylonitrile copolymer
SENT	single-edge notched tensile
WLF	Williams-Landel-Ferry

**Acknowledgement:** R. Lach and W. Grellmann thank the German Federal Ministry of Education and Research (support programme “Wachstums-kern Potenzial”) for financial support within the project “Kombinierte Mikro- und Nanostrukturierung von Kunststoffen” (KoMi-NaKu), subproject 03WKP46E: “Entwicklung quantitativer Testverfahren zur Ermittlung der lokalen mechanischen Eigenschaften beschichteter Folien”.

- [1] K. B. Broberg, *Int. J. Fract.* **1968**, 4, 11.
- [2] B. Cotterell, J. K. Reddel, *Int. J. Fract.* **1977**, 14, 267.
- [3] Y.-W. Mai, B. Cotterell, *Int. J. Fract.* **1986**, 32, 105.
- [4] T. Barany, T. Czigan, J. Karger-Kocsis, *Prog. Polym. Sci.* **2010**, 35, 1257.
- [5] E. Q. Clutton, in *Fracture of Polymers, Composites and Adhesives*,ESIS-Publ. 27, J. G. W. Williams, A. Pavan, Eds., Elsevier, Amsterdam, **2000**, p. 187.
- [6] R. Lach, K. Schneider, R. Weidisch, A. Janke, K. Knoll, *Eur. Polym. J.* **2005**, 41, 383.
- [7] R. Hill, *J. Mech. Phys. Solids* **1952**, 1, 19.
- [8] M. L. Williams, R. F. Landel, J. Ferry, *J. Am. Chem. Soc.* **1955**, 77, 3701.
- [9] E. Donth, *Relaxation and Thermodynamics in Polymers. Glass Transition*, Akademie-Verlag, Berlin, **1992**.
- [10] R. Lach, W. Grellmann, K. Schröter, E. Donth, *Polymer* **1999**, 40, 1481.
- [11] B. Möglinger, G. H. Michler, H.-C. Ludwig, in *Deformation and Fracture Behaviour of Polymers*, W. Grellmann, S. Seidler, Eds., Springer, Berlin Heidelberg, **2001**, p. 335.
- [12] H. G. H. van Melick, *Deformation and Failure of Polymer Glasses*, PhD Thesis, Eindhoven University of Technology, Eindhoven, **2002**.
- [13] J. Karger-Kocsis, J. Moskala, P. P. Shang, *J. Therm. Anal. Calorim.* **2001**, 63, 671.
- [14] J. Karger-Kocsis, T. Czigan, E. J. Moskala, *Polymer* **1998**, 39, 3939.
- [15] R. Quinson, J. Perez, M. Rink, A. Pavan, *J. Mater. Sci.* **1997**, 32, 1371.
- [16] G. H. Michler, *Kunststoff-Mikromechanik. Morphologie, Deformations- und Bruchmechanismen*, Hanser, Munich Vienna, **1992**.
- [17] S. Wu, *Polym. Eng. Sci.* **1990**, 30, 753.
- [18] M. Dettenmaier, Ed., *Crazing in Polymers*, Adv. Polym. Sci. Vol. 52/53, Springer, Berlin, **1983**, p. 57.
- [19] S. Hashemi, J. G. Williams, *Plast. Rubb. Comp.* **2000**, 29, 294.
- [20] S. Hashemi, *J. Mater. Sci.* **1993**, 28, 6178.
- [21] E. C. Y. Ching, R. K. Y. Li, Y.-W. Mai, *Polym. Eng. Sci.* **2000**, 40, 310.
- [22] D. E. Mouzakis, J. Karger-Kocsis, E. J. Moskala, *J. Mater. Sci. Lett.* **2000**, 19, 1615.
- [23] D. E. Mouzakis, *Application of the Essential Work of Fracture Method for Ductile Polymer Systems*, Mensch & Buch Verlag, Berlin, **1999**.
- [24] S. Hashemi, *Polym. Eng. Sci.* **2000**, 40, 798.
- [25] S. Hashemi, *Polym. Eng. Sci.* **2000**, 40, 1435.
- [26] O. F. Yap, Y.-W. Mai, B. Cotterell, *J. Mater. Sci.* **1983**, 18, 657.
- [27] A. Arkhireyeva, S. Hashemi, M. O'Brien, *J. Mater. Sci.* **1999**, 34, 5961.
- [28] G. Levita, L. Parisi, A. Marchetti, L. Bartolommei, *Polym. Eng. Sci.* **1996**, 36, 2534.
- [29] A. S. Saleemi, J. A. Nairn, *Polym. Eng. Sci.* **1990**, 30, 211.
- [30] S. Hashemi, Z. Yuan, *Plast. Rubb. Comp. Process. Applicat.* **1994**, 21, 151.
- [31] C. J. G. Plummer, P. Scaramuzzino, R. Steinberger, R. W. Lang, H.-H. Kausch, *Polym. Eng. Sci.* **2000**, 40, 985.
- [32] G. Levita, L. Parisi, S. McLoughlin, *J. Mater. Sci.* **1996**, 31, 1545.
- [33] W. Y. F. Chan, J. G. Williams, *Polymer* **1994**, 35, 1666.
- [34] J. Wu, Y.-W. Mai, *Polym. Eng. Sci.* **1996**, 36, 2275.
- [35] D. Ferrer, M. L. Maspoch, O. O. Santana, A. B. Martinez, *Revista de Plasticos Modernos* **1997**, 74, 369.

- [36] D. Ferrer-Balas, M. L. Maspocho, A. B. Martinez, O. O. Santana, *Polym. Bull.* **1999**, 42, 101.
- [37] G. Levita, L. Parisi, A. Marchetti, *J. Mater. Sci.* **1994**, 29, 4545.
- [38] D. Arencon, J. I. Velasco, *J. Mater. Sci.* **2001**, 36, 179.
- [39] K. P. Plucknett, V. Normand, *Polymer* **2000**, 41, 6833.
- [40] L. Cousin-Cornet, M. Nait Abdelaziz, G. Mesmacque, C. Cazeneuve, in *Fracture of Polymers, Composites and Adhesives*,ESIS-Publ. 27, J. G. W. Williams, A. Pavan, Eds., Elsevier, Amsterdam, **2000**, p. 201.
- [41] J. D. Ferry, *Viscoelastic Properties of Polymers*, John Wiley & Sons, New York, **1980**.